Journal of Theoretical Biology 257 (2009) 104–115

Contents lists available at ScienceDirect

Journal of Theoretical Biology

journal homepage: www.elsevier.com/locate/yjtbi

Dangerous nutrients: Evolution of phytoplankton resource uptake subject to virus attack

Duncan N.L. Menge [a,*,1], Joshua S. Weitz [b,c,**]

[a] Department of Ecology and Evolutionary Biology, Princeton University, USA
[b] School of Biology, Georgia Institute of Technology, Atlanta, GA 30332, USA
[c] School of Physics, Georgia Institute of Technology, Atlanta, GA 30332, USA

ARTICLE INFO

Article history:
Received 23 June 2008
Received in revised form
3 October 2008
Accepted 21 October 2008
Available online 14 November 2008

Keywords:
Nitrogen
Phosphorus
Model
Stoichiometry
Parasite

ABSTRACT

Phytoplankton need multiple resources to grow and reproduce (such as nitrogen, phosphorus, and iron), but the receptors through which they acquire resources are, in many cases, the same channels through which viruses attack. Therefore, phytoplankton can face a bottom-up vs. top-down tradeoff in receptor allocation: Optimize resource uptake or minimize virus attack? We investigate this top-down vs. bottom-up tradeoff using an evolutionary ecology model of multiple essential resources, specialist viruses that attack through the resource receptors, and a phytoplankton population that can evolve to alter the fraction of receptors used for each resource/virus type. Without viruses present the singular continuously stable strategy is to allocate receptors such that resources are co-limiting, which also minimizes the equilibrium concentrations of both resources. Only one virus type can be present at equilibrium (because phytoplankton, in this model, are a single resource for viruses), and when a virus type is present, it controls the equilibrium phytoplankton population size. Despite this top-down control on equilibrium densities, bottom-up control determines the evolutionary outcome. Regardless of which virus type is present, the allocation strategy that yields co-limitation between the two resources is continuously stable. This is true even when the virus type attacking through the limiting resource channel is present, even though selection for co-limitation in this case decreases the equilibrium phytoplankton population and does not decrease the equilibrium concentration of the limiting resource. Therefore, although moving toward co-limitation and decreasing the equilibrium concentration of the limiting resource often co-occur in models, it is co-limitation, and not necessarily the lowest equilibrium concentration of the limiting resource, that is the result of selection. This result adds to the growing body of literature suggesting that co-limitation at equilibrium is a winning strategy.

1. Introduction

Phytoplankton populations can be regulated by both bottom-up and top-down control. Bottom-up control arises from the influence of limiting nutrients on growth and reproduction (Martin et al., 1994; Vitousek and Howarth, 1991), whereas top-down control results from parasitism (via viruses) (Fuhrman, 1999; Suttle, 2005; Weinbauer, 2004; Wilhelm and Suttle, 1999; Wommack and Colwell, 2000) and/or grazing (Franks, 2002). As well as being regulated by them, phytoplankton populations have important causal impacts on biogeochemical and trophic dynamics, from their pivotal role in ambient nutrient concentrations and Redfield ratios (Karl et al., 2001; Redfield, 1958) to their effects on secondary production in benthic (Menge et al., 1997, 2003) and pelagic (Barber and Chavez, 1983) ecosystems. Quantitative theories of phytoplankton dynamics have long incorporated bottom-up control, the most commonly used of which is the Droop model in which growth is determined by Liebig's law of the minimum for multiple essential nutrients (Ballantyne et al., 2008; Klausmeier et al., 2004; Legović and Cruzado, 1997). The effects of grazing have also been extensively studied, mostly in the context of what are known as NPZ models where N, P and Z denote nutrients, phytoplankton, and zooplankton, respectively (Franks, 2002; Jiang et al., 2005).

In contrast, the influence of parasitism on phytoplankton dynamics and structure is less well understood, but it is increasingly clear that it has a strong impact. Viruses infect, lyse and co-opt phytoplankton (both prokaryotic—such as

* Corresponding author. Tel.: +1 805 882 9218; fax: +1 805 892 2510.
** Corresponding author at: School of Biology, Georgia Institute of Technology, Atlanta, GA 30332, USA. Tel.: +1 404 385 6169; fax: +1 404 894 0519.
E-mail addresses: menge@nceas.ucsb.edu (D.N.L. Menge), jsweitz@gatech.edu (J.S. Weitz).
[1] Current address: National Center for Ecological Analysis and Synthesis, 735 State St., Suite 300, Santa Barbara, CA, 93101, USA.

0022-5193/$ - see front matter © 2008 Elsevier Ltd. All rights reserved.
doi:10.1016/j.jtbi.2008.10.032

cyanobacteria—and eukaryotic phytoplankton), affecting phytoplankton populations, trophic dynamics, and aquatic nutrient cycles (Fuhrman, 1999; Suttle, 2005; Weinbauer, 2004; Wilhelm and Suttle, 1999; Wommack and Colwell, 2000). Viruses can account for a large fraction of phytoplankton mortality. One study calculated that 30% of cyanobacteria mortality resulted from virus lysis (Proctor and Fuhrman, 1990), and others have shown that experimental enrichment of virus concentrations by 20% led to 50% reduction in phytoplankton biomass and primary production (Proctor and Fuhrman, 1992; Suttle, 1992; Suttle et al., 1990). Viruses occur in aquatic environments at densities up to $10^9\,\mathrm{ml}^{-1}$ (Bergh et al., 1989; Suttle et al., 1990; Wilhelm and Suttle, 1999; Wommack and Colwell, 2000), outnumbering prokaryotes by an order of magnitude (Weinbauer, 2004; Wommack and Colwell, 2000) and thus phytoplankton by even more. Some estimates suggest that a quarter of newly photosynthesized carbon in marine environments travels through the "viral shunt," moving it directly to dissolved organic carbon before grazers or other consumers can access it (Suttle, 2005; Wilhelm and Suttle, 1999). Nutrients such as nitrogen, phosphorus, and iron are released from host cells during lysis (Gobler et al., 1997; Poorvin et al., 2004), which is likely to stimulate primary production (Gobler et al., 1997; Poorvin et al., 2004; Weinbauer, 2004; Wilhelm and Suttle, 1999). Virus host range varies from specific (only able to infect a few closely related strains) to broad (able to infect many strains and even multiple "species") (Weinbauer, 2004; Wilhelm and Suttle, 1999; Wommack and Colwell, 2000).

Viruses inject their genetic material into their hosts through receptors on cell surfaces (Fuhrman, 1999; Weinbauer, 2004). Interestingly, some of these receptors, such as certain porins, are the same channels through which nutrients are taken up into phytoplankton cells (Böhm et al., 2001; Gehring et al., 1987; Killmann et al., 1995). This tradeoff between acquiring nutrients and allowing virus attack (Weinbauer, 2004) sets up a number of intriguing evolutionary issues for both the phytoplankton and the viruses. An earlier work (Weitz et al., 2005) used adaptive dynamics modeling to address co-evolutionary changes in bacterial receptors and virus tail fiber configurations for receptors that take up a single limiting nutrient. That study found that selection pressure from viruses drives evolution of bacterial receptors to minimize phage attack at the expense of optimal resource uptake. Concomitant evolution by viruses can allow coexistence of multiple quasispecies of bacteria and of viruses, even for a single limiting nutrient in a homogeneous environment. Recently, the expression of a nutrient uptake receptor (LamB, which controls maltose uptake) in *Escherichia coli* was observed to change in response to top-down pressure from λ-phage (which attack through LamB) (Chapman-McQuiston and Wu, 2008), showing that receptor allocation can be malleable on multiple time scales.

In the present work we address a separate aspect of the bottom-up vs. top-down tradeoff incurred by virus entry through nutrient uptake channels that, to our knowledge, has received little attention. Phytoplankton take up different nutrients through different receptors, and because they need multiple nutrients to survive, they must allocate a fraction of their uptake receptors to each essential nutrient. However, each of these receptors is subject to virus attack (here we only consider virus types that enter through one receptor type), setting up an allocational tradeoff between bottom-up (allocating receptors such that nutrient uptake balances demand) and top-down (allocating receptors such that virus load is minimized) control. We use adaptive dynamics modeling to investigate how selection balances this top-down vs. bottom-up tradeoff, and also to examine the effect of allocation strategies on ambient nutrient concentrations in aquatic ecosystems. In our model, as in others, selection for co-limitation is ubiquitous. For the first time, to our knowledge, we show that selection for co-limitation occurs despite the top-down vs. bottom-up tradeoff. Furthermore, evolution toward co-limitation does not necessarily lower the ambient concentrations of limiting resources, as expected from classic resource competition theory (Tilman, 1982). In the classic case (without top-down pressure), evolution toward co-limitation decreases equilibrium resource concentrations and increases equilibrium phytoplankton population density. However, in an ecological context with a top-down vs. bottom-up tradeoff, evolution toward co-limitation has no effect on equilibrium resource concentrations and actually decreases the equilibrium population density of the phytoplankton.

2. Model and analysis

2.1. Model description

The model we develop and analyze has a population of phytoplankton, multiple essential resources, and viruses that attack through specific nutrient uptake channels. It is general enough that it can be applied to phytoplankton populations in marine or freshwater habitats from tropical, temperate, or boreal latitudes. It could also potentially be applied to other populations that require multiple essential resources, face a top-down tradeoff with the acquisition of each resource, and have evolutionarily flexible allocation for uptake of each resource. The phytoplankton population (B for "biomass") requires all essential resources (R_i) in the model, and can be attacked by all viruses (V_j) in this model. Phytoplankton growth and mortality are influenced by the fraction of receptor allocation devoted to each nutrient uptake channel (x_i), which is the trait we will ultimately allow to evolve. The resources represent the available (typically inorganic) form of essential nutrients, such as nitrate, phosphate, or silicate, and have the essential dynamics common to all such nutrients in real ecosystems, including an input, losses, uptake by the phytoplankton, and recycling. The viruses are specialists that each infect phytoplankton through a specific resource uptake channel; the subscripts of the viruses correspond to the resource with that same subscript. There is evidence that some viruses are generalists (Weinbauer, 2004), entering through generic features of cell membranes such as lipid–polysaccharides, but incorporating generalists into our model yields no qualitatively new results (analysis not shown). Although some viruses can integrate themselves into the chromosomal DNA of their hosts in a latent state (e.g., temperate phages), we focus on viruses that lyse host cells outright. For n resources and viruses, the dynamics of the model are given by

$$\frac{\mathrm{d}B}{\mathrm{d}t} = B\left(g(R_1, R_2, \ldots, R_n) - \left(\mu + \sum_j^n x_j \phi_j V_j\right)\right), \tag{1}$$

$$\frac{\mathrm{d}R_i}{\mathrm{d}t} = I_i - k_i R_i - \frac{B}{\omega_i}\left(g(R_1, R_2, \ldots, R_n) - (1-\delta_i)\left(\mu + \sum_j^n x_j \phi_j V_j\right)\right), \tag{2}$$

$$\frac{\mathrm{d}V_j}{\mathrm{d}t} = V_j(b_j x_j \phi_j B - m_j), \tag{3}$$

$$g(R_1, R_2, \ldots, R_n) = \mathrm{MIN}[x_1\alpha_1 R_1, x_2\alpha_2 R_2, \ldots, x_n\alpha_n R_n]. \tag{4}$$

Because the allocation strategies (x_i) are fractions, they sum to one ($\sum_i^n x_i = 1$), which also indicates the allocational constraint of a fixed number of nutrient uptake receptor sites on a given cell. Phytoplankton growth, Eq. (4), is set by a Liebig's law of the

minimum, a typical formulation for essential resources (e.g., Ballantyne et al., 2008; Klausmeier et al., 2004; Legović and Cruzado, 1997; Tilman, 1982). The relative growth rate (per unit phytoplankton biomass) is the minimum of the relative growth functions for each resource, which are proportional to the concentrations of each resource (R_i), the uptake/growth parameters for each resource (α_i), and the fractions of receptors allocated to taking up each essential nutrient, i.e., the allocation strategies (x_i). These linear functions are simplified approximations of more realistic saturating functions, which we have also examined, and which do not produce qualitatively different results (see Appendix A). Phytoplankton die and enter the nutrient pool due to non-virus-related causes at a constant rate (μ), and due to lysis caused by each virus type (the "viral shunt", as in Suttle, 2005; Wilhelm and Suttle, 1999), which are proportional to the virus population sizes (V_j) and contact rates (ϕ_j). Upon lysis, new viruses are released given by the burst sizes (b_j), and viruses leave the system according to their decay rates (m_j). Nutrients come into the system via constant input fluxes (I_i) and leave via first-order loss rates (k_i). As phytoplankton grow, nutrients are taken up with stoichiometric terms (ω_i), and as phytoplankton die, fractions $(1-\delta_i)$ of the nutrients are mineralized and return to the available nutrient pool, whereas the remaining fractions (δ_i) are lost from the system. The nutrient dynamics in this model are similar to those in other simple ecosystem models (Ballantyne et al., 2008; DeAngelis, 1992; Jiang et al., 2005; Menge et al., 2008), except that uptake also depends on the fraction of receptors allocated to that nutrient. We ignore nutrients cycling through viruses themselves, in part because they do not use some nutrients (such as silicate). The parasite–host dynamics are similar to Type I predator–prey or parasite–host models (Holling, 1959), except for the dependence on the fraction of receptors allocated toward each nutrient.

When limitation is clear we refer to limiting and non-limiting resources and the viruses that attack through those resource channels (R_{lim} and V_{lim} for limiting channels, R_{non} and V_{non} for non-limiting channels). When limitation is unclear we use numbers to distinguish the types. Because the allocation strategies are constrained by summing to one, $n-1$ allocation strategies define the nth strategy. For example, a single allocation strategy defines the other for the case of two resources ($x_{non}=1-x_{lim}$ or $x_2=1-x_1$). A cartoon of our model with two resources is shown in Fig. 1, which shows the allocation strategy (Fig. 1A), the full ecological system (Fig. 1B), and the components of the system (Fig. 1C).

2.2. Model analysis

We analyze this model in two ways. First, we analyze the model as a purely ecological system, finding equilibria and local stability of Eqs. (1)–(3). This provides insight into how the top-down vs. bottom-up tradeoff affects the various components of the system, but leaves unclear how selection will influence the phytoplankton's allocation strategy. To investigate how the tradeoff between nutrient uptake and virus infection plays out evolutionarily, we use techniques from adaptive dynamics (e.g., Geritz et al., 1997). Adaptive dynamics recognizes that the

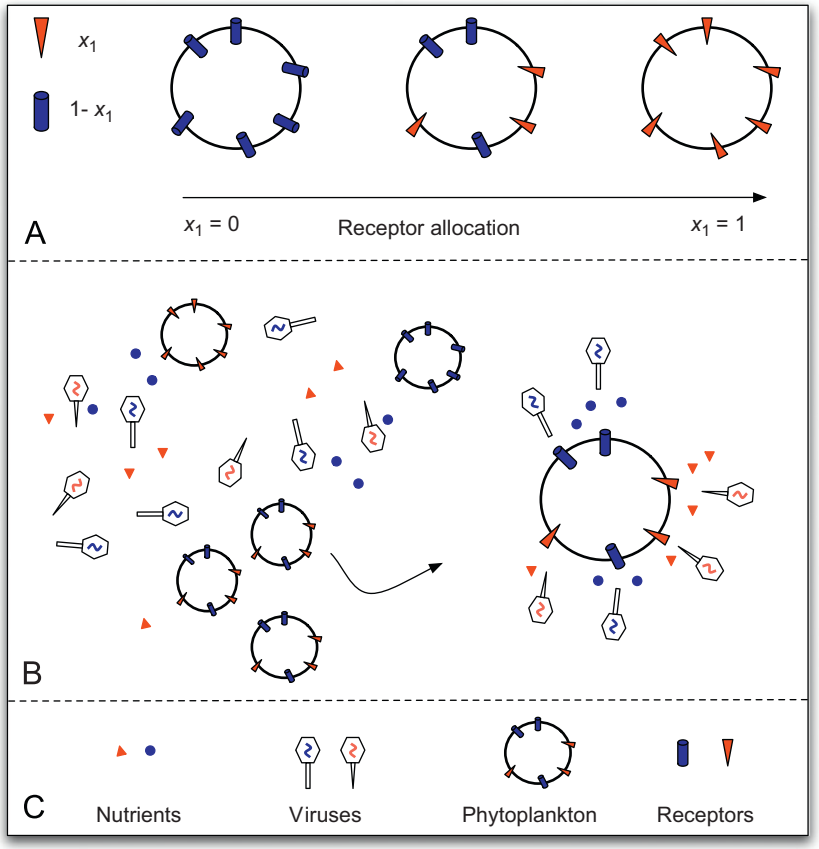

Fig. 1. Cartoon of our model for the case of two receptor types. (A) Phytoplankton strategies are classified according to the fraction of receptors allocated toward uptake of different nutrients. (B) The full model consists of phytoplankton, nutrients, and viruses. Phytoplankton require both essential nutrients for growth and survival, and die due to both viral lysis and non-viral causes. Both nutrients and viruses enter phytoplankton through specific nutrient uptake receptors. (C) Components of the model.

environment—which includes other species and other phenotypes within the focal species—influences evolution, and seeks to determine evolutionary outcomes of model ecosystems. Key assumptions are that ecological dynamics are rapid relative to evolutionary dynamics and that phenotypic evolution sufficiently describes the trait(s) of interest (i.e., there are no genetic limitations to the appearance of mutants near the residents in trait space). In our model, we allow the allocation strategies (x_i) to evolve and we analytically determine evolutionarily stable (cannot be invaded once established) and convergence stable (will be approached from anywhere) strategies (Geritz et al., 1997; Levin and Muller-Landau, 2000; Menge et al., 2008; Weitz et al., 2005).

To illustrate transient dynamics we also simulate the system. Using MATLAB's ode45 function for numerical integration, we simulate the ecological dynamics (Eqs. (1)–(3)) continuously, stopping for certain events. Phytoplankton mutation events occur at a low, exponentially distributed rate. At each mutation event, phytoplankton with different allocation strategies appear at low density. A random draw determines which receptor type switches to which other type, and the degree of difference from their parent type is based on a Gaussian draw with the same mean as the parent. We impose no limit on the number of phytoplankton types that can be in the model, but when the density of a phytoplankton type drops below a threshold (the same as the low density at which they are introduced) we remove them from the model. Viruses do not evolve in our model, but are removed when they reach low enough density in the same way as phytoplankton types. To ensure that all virus types have a chance to succeed, new virus immigrants of all types are introduced at a low, exponentially distributed rate. We simulate the system for two resources and no viruses; two resources and two viruses; and three resources and three viruses. With this exception, all results in the main text are confined to two resources/virus types. In Appendix B we present the extended calculations for n resources and virus types. See Appendix C for simulation parameters and Weitz et al. (2005) for further simulation details.

3. Results

3.1. Ecological analysis

Even though they enter through different channels, different virus types in this model use phytoplankton as their sole resource. As has been noted before (e.g., Tilman, 1982), only one consumer (viruses, in this case) in a homogeneous system can survive in an equilibrium environment. The only exception in this model is at a singular threshold point,

$$\hat{x}_{lim} = \frac{1}{1 + \dfrac{m_{non} b_{lim} \phi_{lim}}{m_{lim} b_{non} \phi_{non}}}, \tag{5}$$

which also defines which virus will win. When phytoplankton allocate more receptors to the limiting resource than this threshold ($x_{lim} > \hat{x}_{lim}$), the virus attacking through the limiting resource channel (V_{lim}) wins, and the top-down vs. bottom-up tradeoff exists. A higher fraction of receptors allocated to the limiting resource (x_{lim}) yields both a higher uptake rate of the limiting resource and a higher rate of virus attack. Alternatively, when phytoplankton allocate less than this threshold to the limiting resource ($x_{lim} < \hat{x}_{lim}$), the other virus (V_{non}) wins and there is no such tradeoff. In this case, a higher fraction of receptors allocated to the limiting resource (x_{lim}) yields a higher uptake rate of the limiting resource, but a lower rate of virus attack, both of which are beneficial to phytoplankton.

For equilibrium calculations we only consider one phytoplankton type. The equilibrium with a top-down vs. bottom-up tradeoff, found by setting Eqs. (1)–(3) equal to zero and specifying that the virus attacking the non-limiting resource channel is absent ($V_{non} = 0$), is

$$\bar{B} = \frac{m_{lim}}{x_{lim} b_{lim} \phi_{lim}}, \tag{6}$$

$$\bar{R}_{lim} = \frac{I_{lim}}{k_{lim} + \dfrac{m_{lim} \delta_{lim} \alpha_{lim}}{b_{lim} \phi_{lim} \omega_{lim}}}, \tag{7}$$

$$\bar{R}_{non} = \frac{1}{k_{non}} \left(I_{non} - \frac{m_{lim} \delta_{non} \alpha_{lim}}{b_{lim} \phi_{lim} \omega_{non}} \bar{R}_{lim} \right), \tag{8}$$

$$\bar{V}_{lim} = \frac{\alpha_{lim}}{\phi_{lim}} \bar{R}_{lim} - \frac{\mu}{x_{lim} \phi_{lim}}. \tag{9}$$

As is generally the case for predator–prey-type models, equilibrium phytoplankton biomass ($\bar{B}$, Eq. (6)) is regulated by the viruses, since it depends on virus parameters. The exception is the allocation strategy (x_{lim}). Even though it increases the uptake rate of the limiting nutrient, increasing the fraction of receptors allocated to the limiting resource (x_{lim}) *decreases* the equilibrium biomass of the phytoplankton ($\bar{B}$, Eq. (6)) because it increases the virus attack rate, further implicating the importance of top-down control on the ecological equilibrium. Increasing the fraction of receptors allocated to the limiting resource (x_{lim}) has no effect on the equilibrium concentrations of either nutrient ($\bar{R}_{lim}$, $\bar{R}_{non}$; Eqs. (7), (8)). Not surprisingly, increasing the fraction of receptors allocated to the limiting resource (x_{lim}) increases the equilibrium virus population size ($\bar{V}_{lim}$, Eq. (9)).

When the virus attacking the limiting resource channel is absent ($V_{lim} = 0$), there is no tradeoff since increasing the fraction of receptors allocated to the limiting resource (x_{lim}) yields both a higher uptake rate of the limiting resource and a lower virus attack rate. This equilibrium is given by

$$\bar{B} = \frac{m_{non}}{(1 - x_{lim}) b_{non} \phi_{non}}, \tag{10}$$

$$\bar{R}_{lim} = \frac{I_{lim}}{k_{lim} + \left(\dfrac{x_{lim}}{1 - x_{lim}} \right) \dfrac{m_{non} \delta_{lim} \alpha_{lim}}{b_{non} \phi_{non} \omega_{lim}}}, \tag{11}$$

$$\bar{R}_{non} = \frac{1}{k_{non}} \left(I_{non} - \left(\frac{x_{lim}}{1 - x_{lim}} \right) \frac{m_{non} \delta_{non} \alpha_{lim}}{b_{non} \phi_{non} \omega_{non}} \bar{R}_{lim} \right), \tag{12}$$

$$\bar{V}_{non} = \frac{x_{lim} \alpha_{lim} \bar{R}_{lim} - \mu}{(1 - x_{lim}) \phi_{non}}. \tag{13}$$

As above, equilibrium phytoplankton biomass is under top-down regulation. Without a tradeoff, increasing the fraction of receptors allocated to the limiting resource (x_{lim}) increases the equilibrium phytoplankton biomass ($\bar{B}$, Eq. (10)) and decreases the equilibrium concentrations of both nutrients ($\bar{R}_{lim}$, $\bar{R}_{non}$; Eqs. (11), (12)). Both equilibria are locally stable when they exist (see Appendix D).

3.2. Evolutionary analysis

3.2.1. Analytical results

It is not intuitively obvious how natural selection will shape allocation to uptake receptors, particularly when the allocational trait carries a tradeoff between top-down and bottom-up forces. With this tradeoff (when the virus attacking the limiting resource channel is present but the other virus is absent), the growth rate of a mutant phytoplankton (B', with allocation strategy x'_{lim}) invading a steady-state system with

a resident (with allocation strategy x_{lim}) is

$$\frac{dB'}{dt} = B'\mu\left(\frac{x'_{lim}}{x_{lim}} - 1\right). \quad (14)$$

Since the mutant's growth rate (dB'/dt) is positive when $x'_{lim} > x_{lim}$, it invades when it allocates a greater fraction of its receptors to the limiting resource than the resident, even though this simultaneously yields a greater mortality rate. This occurs because an increase in the fraction of receptors allocated to the limiting resource (x_{lim}) increases growth more than mortality because there is a component of mortality (μ) that is independent of the allocation strategy (x_{lim}) and viruses (see Eq. (1)). As we show in Appendix E, adding a resource-independent growth term that exceeds the virus-independent mortality term (or removing the virus-independent mortality term) can yield other results. However, because growth must depend on resources, and viruses do not account for all phytoplankton mortality, the biological relevance of these other results is unclear. If growth is limited by a resource that does not require cell-surface receptors, such as light, there is no top-down vs. bottom-up tradeoff for the cell-surface receptor allocation strategy.

When there is no top-down vs. bottom-up tradeoff, selection still pushes the phytoplankton toward co-limitation. The growth rate of a mutant invading a resident when the only virus present is the one attacking the non-limiting resource channel is

$$\frac{dB'}{dt} = B'(\alpha_{lim}\bar{R}_{lim} - \mu)\left(1 - \frac{1 - x'_{lim}}{1 - x_{lim}}\right), \quad (15)$$

where the equilibrium concentration of the limiting resource ($\bar{R}_{lim}$) is set by the resident. Since $x_{lim}\alpha_{lim}\bar{R}_{lim} - \mu > 0$ and $x_{lim} < 1$, the first term in parentheses is positive, and therefore the mutant's growth rate (dB'/dt) is positive when it allocates more receptors to the limiting resource ($x'_{lim} > x_{lim}$). Because the mutant's growth rate (dB'/dt) is positive when it allocates more receptors to the limiting resource ($x'_{lim} > x_{lim}$) regardless of which resource is limiting and which virus is present, selection always pushes the phytoplankton toward co-limitation. Therefore, the allocation strategy that yields co-limitation,

$$x_1^* = \frac{1}{1 + \frac{\alpha_1\bar{R}_1}{\alpha_2\bar{R}_2}} \quad (16)$$

is a convergence stable strategy. Furthermore, the strategy that yields co-limitation (x_1^*) is evolutionarily stable because, once established, any changes to the allocation strategy (x_1) decrease growth, and thus cannot invade. Because it is both convergence and evolutionarily stable, the strategy that yields co-limitation (x_1^*) is a continuously stable strategy (Eshel, 1983). When the top-down vs. bottom-up tradeoff exists ($\hat{x}_1 < x_1^*$ and resource 1 (R_1) is limiting or vice versa), phytoplankton will evolve toward equilibrium co-limitation (x_1^*), even though it decreases equilibrium biomass and does not alter equilibrium concentrations of the limiting resource.

Without any viruses present (i.e., without top-down control), the allocation strategy that gives co-limitation is also continuously stable, as has been seen in a model with flexible stoichiometry (Klausmeier et al., 2007). However, the

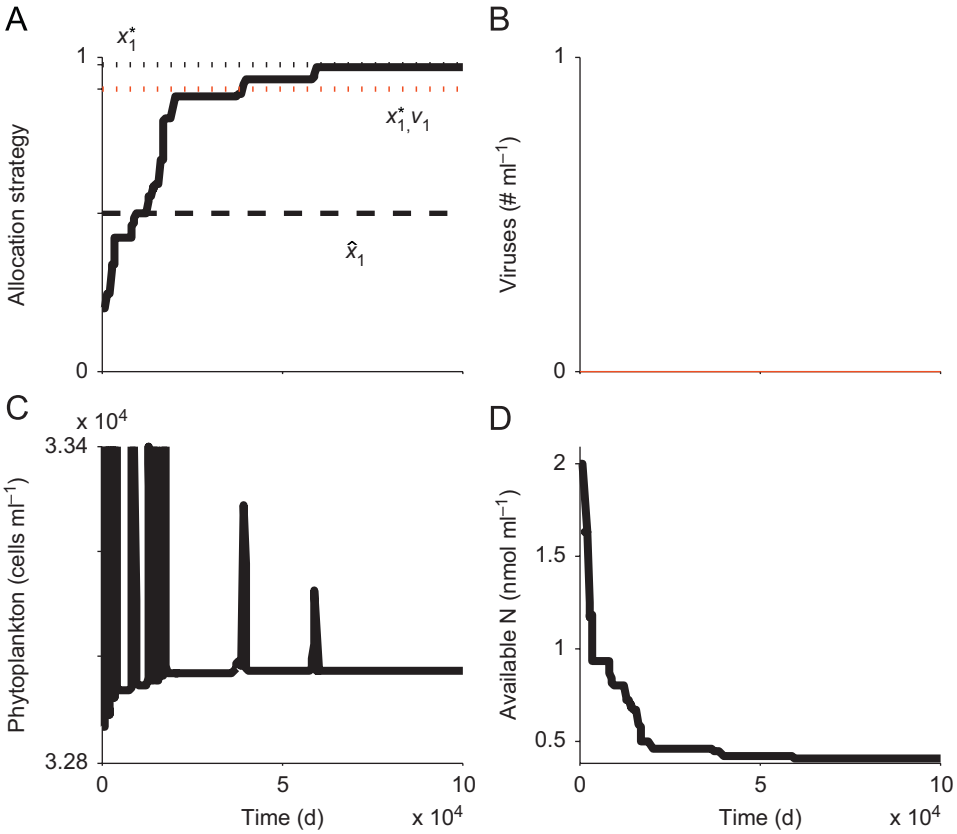

Fig. 2. Evolution with two resources and no viruses. Time is the horizontal axis for all panels, and is on the same scale for all panels. (A) Fraction of receptors allocated toward taking up resource 1 (x_1). The mean of all present individuals is the solid black line. For a population of one quasispecies this is the allocation strategy (x_1) of that quasispecies, but in the transient cases where more than one type exists it is the mean of all types present, weighted by their relative abundance. The black and red dotted lines are the strategies that give co-limitation at equilibrium, with viruses absent (black) and present (red). The dashed black line is the threshold allocation strategy ($\hat{x}_1$) that determines which virus type wins. (B) Virus density. In this simulation both are forced to be zero. (C) Total phytoplankton density (all types are aggregated). Note that higher densities occur but are not shown. (D) Density of resource 1, parameterized as available nitrogen.

co-limitation strategy when viruses are absent is a different strategy than when viruses are present because the equilibrium resource concentrations ($\bar{R}_1$ and $\bar{R}_2$), which determine the co-limitation strategy (x_1^*, Eq. (16)), are different. In this case the co-limitation strategy decreases resource concentrations, as would be expected from resource competition theory (Tilman, 1982). (See Appendix F for these calculations.)

3.2.2. Simulations

Simulations confirm the analytical insights. With viruses absent (Fig. 2) and present (Figs. 3 and 4), the phytoplankton population evolves toward its co-limitation point. However, the co-limitation point is different depending on whether, and which, viruses are present. In Figs. 2A and 3A, the black dotted line represents the co-limitation strategy (x_1^*) without viruses, whereas the red dotted line represents the co-limitation strategy with virus 1 present (x_{1,V_1}^*). The phytoplankton evolve toward the black dotted line in Fig. 2A, but the red dotted line in Fig. 3A. In both cases the allocation strategy (x_1) plotted is the mean of the allocation strategies of all phytoplankton in the ecosystem, but since only one phytoplankton type can exist at equilibrium, the mean is typically the allocation strategy (x_1) of the currently winning type.

When we exclude viruses from the system (Fig. 2), phytoplankton evolution toward the strategy that yields co-limitation (x_1^*) increases equilibrium phytoplankton biomass (Fig. 2C) and lowers resource concentrations (resource 1, parameterized as nitrogen, is shown in Fig. 2D). These results agree with analytical equilibrium calculations (see Appendix F). Each successful mutation causes a transient spike in phytoplankton biomass (up to 5.2×10^4 cells ml^{-1}, off the scale in Fig. 2C).

In the system with two resources and two viruses, which virus type wins depends on the value of the current allocation strategy (x_1) in relation to the threshold allocation strategy ($\hat{x}_1$), as predicted in Eq. (5). At the start of our simulation, the current allocation strategy is below this threshold ($x_1 < \hat{x}_1$), so virus 2 (V_2, blue line in Fig. 3B) wins. Because the current allocation strategy is less than the strategy that yields co-limitation when virus 2 is present ($x_1 < x_{1,V_2}^*$, not shown in Fig. 3A), resource 1 (R_1) is limiting, so there is no top-down vs. bottom-up tradeoff because increasing the fraction of receptors allocated to the limiting resource (x_1) decreases the mortality rate and increases the growth rate. Because the current allocation strategy is below the threshold ($x_1 < \hat{x}_1$), mutants allocating more to the limiting resource (with larger x_1) invade (Fig. 3A), which drives the limiting resource level down (Fig. 3D), increases the equilibrium phytoplankton biomass (Fig. 3C), and decreases the equilibrium virus load (Fig. 3B).

As soon as the current allocation strategy (x_1) crosses the threshold ($\hat{x}_1$), virus 1 (V_1, red line in Fig. 3B) invades and outcompetes virus 2 (V_2), and therefore the top-down vs. bottom-up tradeoff materializes. The phytoplankton population still evolves toward the strategy that yields co-limitation (which is now x_{1,V_1}^*, shown in the red dotted line) (Fig. 3A), but this no longer decreases the equilibrium resource levels (Fig. 3D) and actually decreases the equilibrium phytoplankton population (Fig. 3C), as well as increasing the equilibrium virus load (Fig. 3B). Each successful mutation (jump in Fig. 3A) is accompanied by a transient dip in the resource level (Fig. 3C), but the resource level returns to the same equilibrium.

Similar dynamics are seen in the case with three resources and three viruses (Fig. 4). In this case there are two degrees of freedom for the allocation strategy (x_1 and x_2, so allocation to third

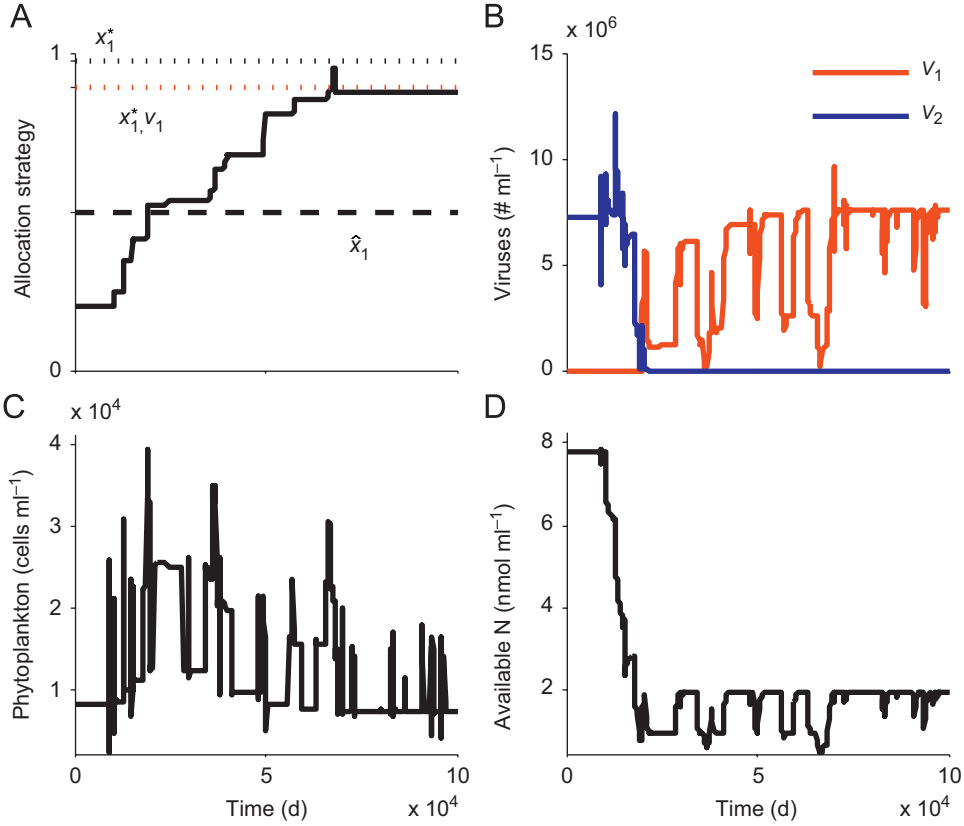

Fig. 3. Evolution with two resources and two viruses. All panels are the same as in Fig. 2, except that in (B) both virus types are shown: virus 1 (V_1) in red, virus 2 (V_2) in blue.

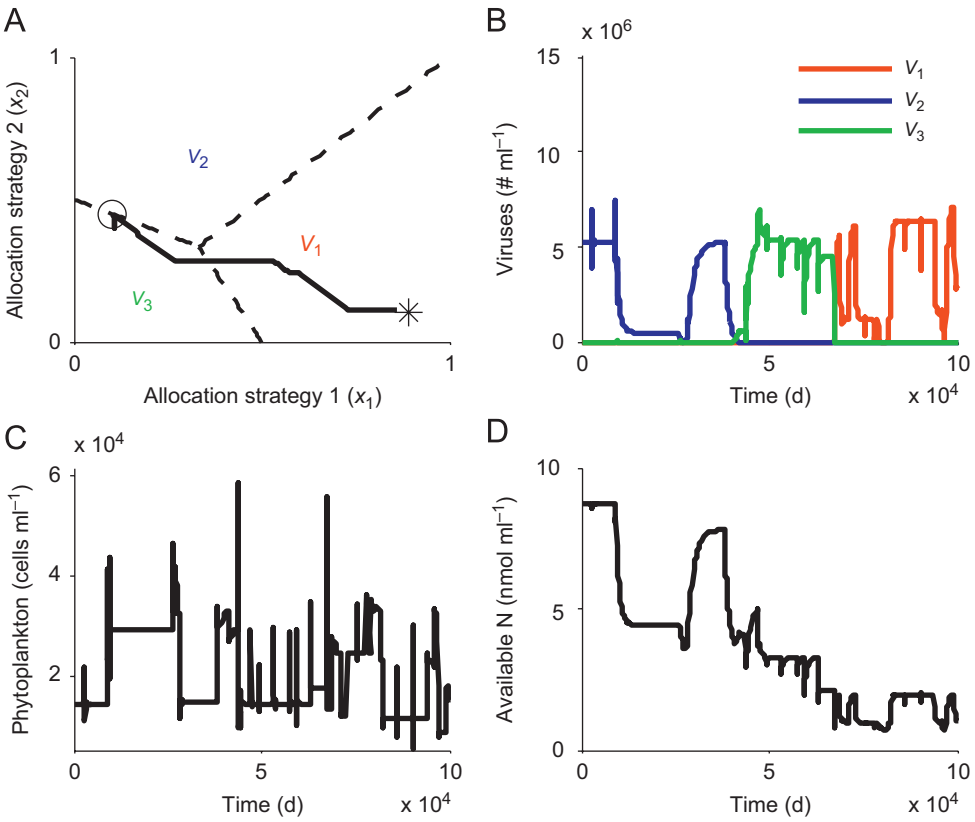

Fig. 4. Evolution with three resources and three viruses. (A) Phase plane diagram of the two allocation strategies (x_1 and x_2). The solid black line is the mean of all present individuals, as in Figs. 2A and 3A. The black dashed lines are thresholds combinations of allocation strategies ($\hat{x}_1$ and $\hat{x}_2$) that determine which virus type wins. Each virus type excludes both the others in one region, indicated by the colored text (V_1, V_2, V_3). The open circle is the starting point, and the black asterisk is the strategy that yields co-limitation between all three resources when virus 1 (V_1) is present. (B) Same as Fig. 3, except that there are now three virus types (corresponding to three essential resources). (C) and (D) are the same as in Figs. 2 and 3.

resource is $1 - x_1 - x_2$), so Fig. 4A is a phase plane diagram with allocation strategy 1 (x_1) on the horizontal axis and allocation strategy 2 (x_2) on the vertical axis. The strategy space is divided into three regions by threshold lines (dashed black lines derived in Appendix B, similar to the threshold strategy $\hat{x}_1$ in Fig. 3A) that determine which virus type wins (indicated by colored text). The simulation begins (the open circle in Fig. 4A) in the region where virus 2 wins, as shown in Fig. 4B. The phytoplankton population soon crosses into the region where virus 3 wins, and eventually into the region where virus 1 wins (Fig. 4A,B). Throughout, the phytoplankton population evolves toward the strategy set that yields co-limitation by all three resources. The strategy that yields co-limitation with virus 1 present (derived in Appendix B) is shown in Fig. 4A with a black asterisk. With virus 1 present and resource 1 limiting, the top-down vs. bottom-up tradeoff materializes. With this tradeoff, the phytoplankton equilibrium population decreases (Fig. 4C) and the equilibrium nutrient density remains constant (Fig. 4D), as in the case with two resources.

4. Discussion

There has been much debate in the ecological literature about the importance of bottom-up vs. top-down factors (Borer et al., 2006; Hairston et al., 1960; Hunter et al., 1997; Menge, 2000; Vitousek and Howarth, 1991). Our model incorporates both types of pressure on a phytoplankton population—phytoplankton need essential resources to grow, and can be killed by viruses—and thus can be used to ask questions about which factors are important drivers of particular patterns. As has been known for a long time in predator–prey or parasite–host models (e.g., Rosenzweig and MacArthur, 1963), the phytoplankton (prey) population is controlled by top-down pressure at the ecological equilibrium. However, bottom-up factors are the target of selection over evolutionary time scales, even when bottom-up and top-down forces are in direct conflict for the evolving trait. Hence, the fraction of resource uptake receptors allocated toward the limiting resource increases over evolutionary time, even when viruses can only enter through that receptor type, and this evolutionary change both decreases equilibrium phytoplankton density and has no effect on equilibrium nutrient density.

This result adds to the growing body of literature that argues that both bottom-up and top-down factors are important (e.g., Hunter et al., 1997; Jaschinski and Sommer, 2008; Jiang et al., 2005; Menge, 2000; Menge et al., 1997, 1999, 2003; Moreau et al., 2006). Some of these studies have shown that bottom-up and top-down factors are important on different spatial scales (Menge, 2000; Menge et al., 1997, 1999, 2003), and our study adds a new wrinkle of different time scales (top-down for ecological, bottom-up for evolutionary time scales).

Selection for the strategy that yields co-limitation at equilibrium is ubiquitous in our model, even when this selection decreases phytoplankton biomass and does not alter nutrient concentrations at equilibrium. This result strengthens an argument put forth by Klausmeier et al. (2007) that selection for the unique allocation strategy that leads to co-limitation should be thought of as a general principle. This has now been shown in

models of general consumers needing two essential resources (Abrams, 1987; Tilman, 1982), plants that need light and nutrients (Reynolds and Pacala, 1993), bacteria with two essential resources (Van den Berg et al., 2002), and phytoplankton with two (Klausmeier et al., 2007; the present work) or more (the present work) essential resources. These models differ in many ways, including stoichiometry (static vs. flexible), techniques (optimization vs. adaptive dynamics), resource dynamics (e.g., nutrients vs. light, including recycling or not), functional responses (e.g., linear vs. saturating resource uptake), and the presence of top-down pressure on the evolving trait, in which our model is unique among those cited above. Our work is perhaps the most robust test of this general principle, given that there is a direct tradeoff between evolving toward co-limitation and increased mortality.

In an interesting departure from these other models, our model shows that evolution toward co-limitation is not synonymous with decreasing the equilibrium concentration of the limiting resource (the R^* principle of Tilman, 1982). As can be seen in Fig. 3D, each successful mutation is accompanied by a transient decrease in the limiting nutrient concentration, but in the case where there is a top-down vs. bottom-up tradeoff (after virus 1 takes over from virus 2 or virus 3, seen in Figs. 3B and 4B), the equilibrium concentration of the limiting resource is the same (as can be seen in Eq. (7)). Therefore, co-limitation at equilibrium, rather than the minimum equilibrium resource concentration, is the target of selection. In many models, moving toward co-limitation and decreasing the equilibrium concentration of the limiting resource co-occur, but our model demonstrates an exception.

Co-limitation by multiple resources seems to be common in many real ecosystems (Elser et al., 2007), seemingly in agreement with this model result. However, some studies testing for multiple resource limitation reveal a response to only a single factor (e.g., Dukes et al., 2005; Vitousek and Farrington, 1997), and it is unclear from meta-analyses that reveal community-level co-limitation whether individual species are co-limited (as these models predict) or whether community-level co-limitation arises from multiple species being limited by a single (but different) resource each (Elser et al., 2007). Therefore, co-limitation of individual species in natural ecosystems may not be ubiquitous. Given the robustness of the model prediction of co-limitation, what could cause single resource limitation? In our model, and in the models cited earlier, allocation to resource uptake is flexible, either over physiological (for optimization models) or evolutionary time. If allocation is not flexible, i.e., if there are inherent constraints on allocation patterns (as for nitrogen fixation in Menge et al., 2008), single resource limitation could result. However, the biological basis of such constraints for receptor allocation is unclear.

Another possible explanation for single resource limitation is a non-steady-state environment. If resource availability changes on a faster time scale than autotrophs' ability to alter allocation, single resource limitation could be pervasive. Changing resource availability could result from external forcing (such as climatic/oceanographic patterns or disturbance), and could also result from the system itself. Many predator–prey-type models predict oscillations, some of which persist indefinitely and some of which die away without perturbation (e.g., Rosenzweig and MacArthur, 1963; Volterra, 1926). For the parameters we used there are no oscillations in our model (although exploration of parameter space shows that damped oscillations are possible), but each mutation perturbs the system relatively far away from equilibrium (as seen in the apparent fluctuations in virus, phytoplankton, and resource densities). Therefore, if evolutionary processes (successful mutations) are sufficiently rapid relative to ecological processes (return to ecological equilibrium), they could maintain single resource limitation indefinitely.

Throughout this paper we have focused on phytoplankton and the viruses that attack them, but our model applies equally well to other single-celled organisms that acquire multiple essential resources through virus-prone receptors. For instance, heterotrophic prokaryotes in aquatic systems, which play key roles in biogeochemical cycling (Azam et al., 1983; Cho and Azam, 1988) and are highly prone to virus infection (Fuhrman, 1999; Suttle, 2005; Weinbauer, 2004; Wilhelm and Suttle, 1999; Wommack and Colwell, 2000), require multiple essential resources to survive (such as carbon and nutrient sources), and it is likely they face a similar top-down vs. bottom-up tradeoff. Our model could also be applied to multicellular organisms that face similar tradeoffs, such as being infected by different food-borne parasites in different essential food sources.

Acknowledgments

We are pleased to acknowledge the support of the Defense Advanced Research Projects Agency under Grant HR0011-05-1-0057 to Princeton University and an NSF Graduate Research Fellowship (to D.N.L.M.). Joshua Weitz, Ph.D., holds a Career Award at the Scientific Interface from the Burroughs Wellcome Fund. We thank Simon Levin, Steve Pacala, Ford Ballantyne, and the members of the Theoretical Ecology Group at Princeton University, where this work was initiated, for many inspiring discussions.

Appendix A. Results with saturating functions

Using the growth function

$$g(R_1,R_2,\ldots,R_n)=\mathrm{MIN}\left[\frac{x_1\alpha_1R_1}{\beta_1+R_1},\frac{x_2\alpha_2R_2}{\beta_2+R_2},\ldots,\frac{x_n\alpha_nR_n}{\beta_n+R_n}\right] \tag{A.1}$$

instead of Eq. (4), the equilibria are as follows. With V_{lim} present,

$$\bar{B}=\frac{m}{xb\phi}, \tag{A.2}$$

$$\bar{R}_{lim}=\frac{1}{2k}\left[I-\frac{m\delta\alpha}{b\phi\omega}-k\beta+\sqrt{\left(I-\frac{m\delta\alpha}{b\phi\omega}-k\beta\right)^2+4kI\beta}\right], \tag{A.3}$$

$$\bar{R}_{non}=\frac{1}{k_{non}}\left[I_{non}-\frac{m\delta_{non}\alpha\bar{R}_{lim}}{\omega_{non}b\phi(\beta+\bar{R}_{lim})}\right], \tag{A.4}$$

$$\bar{V}_{lim}=\frac{\alpha\bar{R}_{lim}}{\phi(\beta+\bar{R}_{lim})}-\frac{\mu}{x\phi}, \tag{A.5}$$

where all parameters have the subscript $_{lim}$ (omitted for brevity) unless otherwise noted (and except μ, which has no receptor distinction). As in the linear case, $\bar{B}$ decreases with x_{lim}, $\bar{V}_{lim}$ increases, and both $\bar{R}_{lim}$ and $\bar{R}_{non}$ do not change.

With V_{non} present,

$$\bar{B}=\frac{m_{non}}{b_{non}\phi_{non}(1-x)}, \tag{A.6}$$

$$\bar{R}_{lim}=\frac{1}{2k}\left[Y+\sqrt{Y^2+4kI\beta}\right], \tag{A.7}$$

$$Y=I-\left(\frac{x}{1-x}\right)\frac{m_{non}\delta\alpha}{b_{non}\phi_{non}\omega}-k\beta, \tag{A.8}$$

$$\bar{R}_{non} = \frac{1}{k_{non}}\left[I_{non} - \left(\frac{x}{1-x}\right)\frac{m_{non}\delta_{non}\alpha\bar{R}_{lim}}{\omega_{non}b_{non}\phi_{non}(\beta+\bar{R}_{lim})}\right], \tag{A.9}$$

$$\bar{V}_{non} = \left(\frac{x}{1-x}\right)\frac{\alpha\bar{R}_{lim}}{\phi_{non}(\beta+\bar{R}_{lim})} - \frac{\mu}{\phi_{non}(1-x)}, \tag{A.10}$$

where, again, all parameters have the subscript $_{lim}$ unless otherwise noted. As with the linear functions, $\bar{B}$ increases with x_{lim} and both $\bar{R}_{lim}$ and $\bar{R}_{non}$ decrease.

The invasion conditions with saturating growth functions are very similar to those with linear functions. When V_{lim} is present the growth rate of an invading type B' is exactly the same as Eq. (14), whereas when V_{non} is present it is

$$\frac{dB'}{dt} = B'\left(\frac{\alpha_{lim}\bar{R}_{lim}}{\beta_{lim}+\bar{R}_{lim}} - \mu\right)\left(1 - \frac{1-x'_{lim}}{1-x_{lim}}\right), \tag{A.11}$$

which, as in the linear case, is positive when $x'_{lim} > x_{lim}$.

Appendix B. Results for more than two resources and viruses

With n resource and virus types, there are $n-1$ degrees of freedom for the allocation strategies x_i. Therefore, there are theoretically many possible types of mutations, such as increasing x_1 while decreasing x_2 and leaving all others constant, increasing x_1 while decreasing $x_2 \ldots x_n$ equally, increasing x_1 and x_2 while decreasing x_3, and so on. Biologically, the mutations of interest are switches from one receptor type to another, so we confine our analysis here to simple switches from one receptor type to another receptor type.

The singular point that allows co-existence of multiple virus types is a simple extension of Eq. (5),

$$x_i = \frac{1}{\sum_j^n \frac{m_j b_i \phi_i}{m_i b_j \phi_j}} \tag{B.1}$$

for every x_i. This is also the intersection of the lines that determine which virus type can invade which other virus type. Virus i can invade virus j when

$$x_i > \frac{m_i b_j \phi_j}{m_j b_i \phi_i} x_j, \tag{B.2}$$

leading to regions of strategy space in which one virus type excludes all others. These are the three regions denoted in Fig. 4A.

Equilibrium calculations with n types are very similar to those for two types. When the virus attacking the limiting resource channel is present, the equilibrium expressions are exactly the same as Eqs. (6)–(9) (or Eqs. (A.2)–(A.5) for the saturating uptake case), where $\bar{R}_{non}$ represents all non-limiting resources (with parameters subscripted "*non*" being the parameters for that particular R_{non}). When the virus present is attacking a non-limiting resource channel, some subscripts change. With more than two types, all "*non*" subscripts in Eqs. (10)–(13) (or Eqs. (A.6)–(A.10) for the saturating uptake case) refer to the channel through which the virus is attacking (and $1-x_{lim}$ becomes the x_{non} for this channel), except for the equations for non-limiting resources through which no virus is attacking. If "non,V" refers to the channel through which the virus is attacking and "non,j" refers to the all other non-limiting resource channels j, the equilibrium value of the non-limiting resources that have no virus attacking are

$$\bar{R}_{non,j} = \frac{1}{k_{non,j}}\left(I_{non,j} - \left(\frac{x_{lim}}{x_{non,V}}\right)\frac{m_{non,V}\delta_{non,j}\alpha_{lim}}{b_{non,V}\phi_{non,V}\omega_{non,j}}\bar{R}_{lim}\right) \tag{B.3}$$

for the linear case (the saturating case is analogous).

Local stability (see Appendix D) also extends to n types. The non-limiting resource columns in the Jacobian matrix have all zeros except for their diagonal term, which is $-k_{non}$. Therefore, the upper left 3×3 submatrix is the same as in Appendix D, the upper right submatrix is all zeros (so the whole matrix is triangular), and the lower right submatrix has all zeros except for negative terms on the diagonal. Triangularity means that the eigenvalues of the whole matrix are the eigenvalues of the upper left and lower right submatrices. Because the upper left submatrix is the same as in Appendix D, all its eigenvalues are negative. Because the lower right submatrix is itself triangular, its eigenvalues are the diagonal elements, which are all negative. Therefore, the system with n resources is locally stable. (Analogous results hold for equilibrium and stability calculations for the case of no viruses, as in Appendix F.)

With more than two resources and viruses, the evolutionary analysis must consider the potential mutation of any of the allocation strategies (x_i). When the top-down vs. bottom-up tradeoff exists (i.e., when the virus attacking the limiting resource channel is present but all others are absent), the invasion of a mutant allocating more or less to the limiting resource (x'_{lim} invading x_{lim}) is exactly the same as Eq. (14), so that strategy will evolve toward co-limitation despite decreasing equilibrium phytoplankton biomass and not changing equilibrium resource densities, as was the case for two resources and viruses. Mutants allocating more or less to a non-limiting resource but leaving allocation to the limiting resource unchanged ($x'_{non} \neq x_{non}$ but $x'_{lim} = x_{lim}$) when the top-down vs. bottom-up tradeoff exists have neutral invasion terms. However, even genetic drift could push the phytoplankton toward co-limitation because a non-limiting resource (the one with less allocation to it) would become closer to being limiting (although the one with more allocation to it would become farther from being limiting).

If the virus present is attacking a non-limiting resource channel, there is no top-down vs. bottom-up tradeoff, and co-limitation is still selected for. In this case there are four possible mutations of interest: (i) a switch between the fractions of receptors allocated to the limiting resource (x_{lim}) and the non-limiting resource with the virus present ($x_{non,V}$), (ii) a change in x_{lim} with no change in $x_{non,V}$, (iii) a change in $x_{non,V}$ with no change in x_{lim}, and (iv) a change in other allocation strategies with no change in x_{lim} or $x_{non,V}$. Case (i) is analogous to the main text (Eq. (14)), but now $x_{non,V} = 1 - \sum_j^{n;j\neq non,V;j\neq lim} - x_{lim}$, and $x_{non,V}$ and x_{lim} are the only strategies changing. Using the shorthand $\sum_j^{n;j\neq non,V;j\neq lim} x_j = \sum_j x_j$, the invasion equation is now

$$\frac{dB'}{dt} = B'\left(\alpha_{lim}\bar{R}_{lim}\left(1 - \sum_j x_j\right) - \mu\right)\left(1 - \frac{1-\sum_j x_j - x'_{lim}}{1-\sum_j x_j - x_{lim}}\right). \tag{B.4}$$

As in Eq. (15), Eq. (B.4) is positive when $x'_{lim} > x_{lim}$, so selection leads to co-limitation.

For case (ii), the invasion equation is

$$\frac{dB'}{dt} = B'(\mu + x_{non,V}\phi_{non,V}\bar{V}_{non,V})\left(\frac{x'_{lim}}{x_{lim}} - 1\right). \tag{B.5}$$

Because the expression in the first parentheses is always positive, mutants allocating more to the limiting resource always invade, as before. For case (iii), the invasion equation is

$$\frac{dB'}{dt} = B'(x_{lim}\alpha_{lim}\bar{R}_{lim} - \mu)\left(1 - \frac{x'_{non,V}}{x_{non,V}}\right). \tag{B.6}$$

In this case, mutants allocating less to the non-limiting resource invade. This pushes the phytoplankton toward co-limitation because less allocation to a non-limiting resource will eventually lead to co-limitation between this resource and the formerly limiting resource. In this case, the top-down pressure is the only

pressure under selection. In case (iv), invasion is neutral, as above. As a whole, these results show that directional evolution of the fractions of receptors allocated to the limiting or non-limiting resources always push the phytoplankton population toward co-limitation between all essential resources, possibly passing through co-limitation between subsets of all essential resources.

The strategy the yields co-limitation between all resources,

$$x_i^* = \frac{1}{\sum_j^n \frac{\alpha_i \bar{R}_i}{\alpha_j \bar{R}_j}} \tag{B.7}$$

for all x_i, is a continuously stable strategy, analogous to the two resource/virus case in the main text. This strategy, solved for three resources (with two degrees of freedom) and virus 1 present, is the co-limitation point plotted in Fig. 4A toward which evolution proceeds.

Appendix C. Simulation parameters

The equations we use for the ecological model in the simulations are the same as Eqs. (1)–(3), except we allow for the possibility of multiple phytoplankton types B_k with different allocation strategies x_{ik} to nutrient R_i. Parameter values are in Table C1.

Appendix D. Stability of ecological equilibria

The Jacobian for the system with V_{lim}, ordered dV_{lim}/dt, dB/dt, dR_{lim}/dt, dR_{non}/dt, is

$$\begin{pmatrix} 0 & b(x\alpha\bar{R}_{lim}-\mu) & 0 & 0 \\ -\frac{m}{b} & 0 & \frac{\alpha m}{b\phi} & 0 \\ \frac{(1-\delta)m}{\omega b} & -\frac{\delta x\alpha\bar{R}_{lim}}{\omega} & -k-\frac{\alpha m}{\omega b\phi} & 0 \\ \frac{(1-\delta_{non})m}{\omega_{non}b} & -\frac{\delta_{non}x\alpha\bar{R}_{lim}}{\omega_{non}} & -\frac{\alpha m}{\omega_{non}b\phi} & -k_{non} \end{pmatrix}, \tag{D.1}$$

where all parameters are for the limiting resource channel unless otherwise specified. When divided into two blocks, with dividing lines between the third and fourth rows and the third and fourth columns, this is a triangular matrix, so the eigenvalues of the two blocks are the eigenvalues of the full matrix. The lower right eigenvalue, $-k_{non}$, is negative. Thus, negative eigenvalues of the upper left block (for dV_{lim}/dt, dB/dt, and dR_{lim}/dt) guarantee local stability of the full system. All eigenvalues are negative when the opposite of the trace (−Tr), the sum of principal minors (which we will call □), and the opposite of the determinant (−Det), of the upper left block are all positive; and $-\mathrm{Tr}\square > -\mathrm{Det}$.

$$-\mathrm{Tr} = \left(k+\frac{\alpha m}{\omega b\phi}\right), \tag{D.2}$$

$$\square = m(x\alpha\bar{R}_{lim}-\mu)+\frac{\alpha^2 m\delta x\bar{R}_{lim}}{\omega b\phi}, \tag{D.3}$$

$$-\mathrm{Det} = m(x\alpha\bar{R}_{lim}-\mu)\left(k+\frac{\delta\alpha m}{\omega b\phi}\right). \tag{D.4}$$

Since $\delta<1$, the equilibrium is locally stable when it exists.

The Jacobian for system with V_{non}, ordered dV_{non}/dt, dB/dt, dR_{lim}/dt, dR_{non}/dt, is

$$\begin{pmatrix} 0 & b_{non}(x\alpha\bar{R}_{lim}-\mu) & 0 & 0 \\ -\frac{m_{non}}{b_{non}} & 0 & \left(\frac{x}{1-x}\right)\frac{\alpha m_{non}}{b_{non}\phi_{non}} & 0 \\ \frac{(1-\delta)m_{non}}{\omega b_{non}} & -\frac{\delta x\alpha\bar{R}_{lim}}{\omega} & -k-\left(\frac{x}{1-x}\right)\frac{\alpha m_{non}}{\omega b_{non}\phi_{non}} & 0 \\ \frac{(1-\delta_{non})m_{non}}{\omega_{non}b_{non}} & -\frac{\delta_{non}x\alpha\bar{R}_{lim}}{\omega_{non}} & -\left(\frac{x}{1-x}\right)\frac{\alpha m_{non}}{\omega_{non}b_{non}\phi_{non}} & -k_{non} \end{pmatrix}, \tag{D.5}$$

where, again, all parameters are for the limiting resource channel unless otherwise specified. The same analysis from above holds,

Table C1
Parameters in model simulations.

Symbol	Definition	Units	Value 1[a]	Value 2
u	Mutation probability	–	1×10^{-6}	5×10^{-8}
u_{σ^2}	Variance of mutation size	–	0.004	0.01
D_{cut}	Density cutoff threshold	Cells or viruses ml^{-1}	0.0001	–
D_{new}	New density	Cells or viruses ml^{-1}	0.0001	–
ρ	Immigration rate	d^{-1}	0.01	–
α	Nutrient uptake rate[b,c]	$(\mathrm{mmol\,R\,ml^{-1}})^{-1}\,d^{-1}$	5×10^{4}	8.3×10^{6}
μ	Phytoplankton death rate[b]	d^{-1}	0.2	–
δ	Fraction mortality not recycled[b]	–	0.05	0.05
ω	Phytoplankton R use efficiency[d]	Cells $\mathrm{mmol\,R^{-1}}$	6.6×10^{10}	1.06×10^{12}
m	Virus decay rate[e]	d^{-1}	0.1	0.1
b	Burst size[e]	Viruses $cell^{-1}$	150	150
ϕ	Virus contact rate[f]	$(\mathrm{Viruses\,ml^{-1}})^{-1}\,d^{-1}$	1×10^{-7}	1×10^{-7}
I	Nutrient input flux[f]	$\mathrm{mmol\,R\,ml^{-1}\,d^{-1}}$	5×10^{-9}	3.2×10^{-10}
k	Nutrient loss rate	d^{-1}	1×10^{-5}	1×10^{-5}

R_1 is parameterized as nitrogen (where the available form is $NO_3^- + NO_2^- + NH_4^+$) and R_2 as phosphorus (available form PO_4^{3-}). For the simulation with three resources and viruses, parameters for type three were midpoints between those for types 1 and 2.

[a] Values 1 and 2 refer to resources R_1 and R_2 and/or virus types V_1 and V_2, except for u and u_{σ^2}, where value 1 is for the virus-free simulation and value 2 is for the simulations with viruses.

[b] From Tyrrell (1999), with unit conversions where necessary.

[c] Maximum rates from saturating curve.

[d] From Redfield ratios (C:N:P of 106:16:1, Redfield, 1958) and 10 cells $\mathrm{pmol\,C^{-1}}$ (Li, 2002).

[e] From De Paepe and Taddei (2006).

[f] Calculated using Eqs. (6)–(8), equilibrium biomass of 10^4 cells ml^{-1} from Wilhelm and Suttle (1999), surface nutrient values of 2 $\mathrm{nmol\,N\,ml^{-1}}$ and 0.15 $\mathrm{nmol\,P\,ml^{-1}}$ from Levitus et al. (1993) and Tyrrell (1999), and fixed k's, with N as the limiting nutrient.

except that now

$$-\mathrm{Tr} = \left(k + \left(\frac{x}{1-x}\right)\frac{\alpha m_{non}}{\omega b_{non}\phi_{non}}\right), \tag{D.6}$$

$$\square = m_{non}(x\alpha\bar{R}_{lim} - \mu) + \left(\frac{x}{1-x}\right)\frac{\alpha^2 m_{non}\delta x\bar{R}_{lim}}{\omega b_{non}\phi_{non}}, \tag{D.7}$$

$$-\mathrm{Det} = m_{non}(x\alpha\bar{R}_{lim} - \mu)\left(k + \left(\frac{x}{1-x}\right)\frac{\delta\alpha m_{non}}{\omega b_{non}\phi_{non}}\right). \tag{D.8}$$

As above, since $\delta<1$, the equilibrium is locally stable when it exists (see May, 1973 for details of these analyses).

Appendix E. Effect of constant growth term on results

In our original model the basic evolutionary result is that co-limitation is selected for, even when there is a top-down vs. bottom-up tradeoff that results in lower equilibrium biomass and no change in equilibrium resource concentrations as co-limitation is approached. Mathematically, this result stems from the fact that there is a component of mortality unrelated to the fraction of receptors allocated to the limiting resource (x_{lim}), μ, whereas there is no such component for growth. Biologically, the meaning of adding such a component for growth or removing the virus-independent mortality term would be unclear, because growth must depend on limiting resources and not all phytoplankton mortality stems from viruses. For the purposes of mathematical illustration, however, we now demonstrate that adding a constant growth term (γ) to the growth equation or removing the constant mortality term (μ) can alter the results. With both constant growth and mortality terms, the phytoplankton growth equation is

$$\frac{dB}{dt} = B\left((\gamma + g(R_1, R_2, \ldots, R_n)) - \left(\mu + \sum_j^n x_j\phi_j V_j\right)\right). \tag{E.1}$$

For there to be a top-down vs. bottom-up tradeoff, let V_{lim} be present. At equilibrium,

$$\alpha_{lim}\bar{R}_{lim} = \frac{\mu}{x_{lim}} + \phi_{lim}\bar{V}_{lim} - \frac{\gamma}{x_{lim}}, \tag{E.2}$$

so the mutant's growth rate would be

$$\frac{dB'}{dt} = B'(\mu - \gamma)\left(\frac{x'_{lim}}{x_{lim}} - 1\right). \tag{E.3}$$

Eq. (E.3) reveals that, if there are constant growth and mortality terms, mutants allocating more than the residents to the limiting resource ($x'_{lim} > x_{lim}$) will only invade when the constant mortality term (μ) is greater than the constant growth term (γ). If the constant growth term exceeds the constant mortality term ($\gamma > \mu$), mutants allocating more to the non-limiting resource ($x'_{lim} < x_{lim}$) would invade, and evolution would proceed away from co-limitation. If there were neither a constant growth term nor a constant mortality term, the mutant's invasion growth rate would be zero (see Eqs. (14), (E.3) when $\mu = 0$ and $\gamma = 0$). However, neither of these cases is biologically realistic since there is no component of growth that does not depend on limiting resources, and there is always virus-independent mortality.

Appendix F. Results without viruses

F.1. Equilibrium and stability conditions

Without any viruses, the equilibrium for a linear uptake function is given by

$$\bar{B} = \frac{\omega_{lim}}{\mu\delta_{lim}}\left(I_{lim} - \frac{k_{lim}\mu}{x_{lim}\alpha_{lim}}\right), \tag{F.1}$$

$$\bar{R}_{lim} = \frac{\mu}{x_{lim}\alpha_{lim}}, \tag{F.2}$$

$$\bar{R}_{non} = \frac{1}{k_{non}}\left(I_{non} - \frac{\bar{B}\mu\delta_{non}}{\omega_{non}}\right). \tag{F.3}$$

Local stability of the system without viruses is guaranteed by the sign structure of the Jacobian matrix, which is

$$\begin{pmatrix} 0 & + & 0 \\ - & - & 0 \\ - & 0 & - \end{pmatrix}. \tag{F.4}$$

The eigenvalues of this triangular matrix are given by the (3,3) entry (which is negative) and the eigenvalues of the 2×2 matrix in the upper left. The eigenvalues of the upper left matrix are negative because the trace is negative and the determinant is positive (Routh–Hurwitz conditions for a 2×2 matrix). Therefore, all eigenvalues are negative, so the ecosystem is locally stable. See May (1973) for details of this linearization analysis.

F.2. Co-limitation is continuously stable

Invasion of a mutant type under single resource limitation is given by

$$\frac{dB'}{dt} = B'\mu\left(\frac{x'_{lim}}{x_{lim}} - 1\right), \tag{F.5}$$

exactly the same as in the case where viruses attacking the limiting resource channel are in the system. Therefore, mutants allocating more toward taking up the limiting resource invade.

Invasions will push the system toward the strategy that yields co-limitation at equilibrium. This point is given by the strategy x_1^* that satisfies $x_1\alpha_1\bar{R}_1 = (1-x_1)\alpha_2\bar{R}_2$, which is given by the positive root of the quadratic equation

$$x_1^{*2}(C_3I_1 - I_2) + x_1^*(I_2 - C_2 - C_3C_1 - C_3I_1) + C_3C_1 = 0, \tag{F.6}$$

where

$$C_1 = \frac{\mu k_1}{\alpha_1}, \tag{F.7}$$

$$C_2 = \frac{\mu k_2}{\alpha_2}, \tag{F.8}$$

$$C_3 = \frac{\omega_1\delta_2}{\omega_2\delta_1}. \tag{F.9}$$

To determine whether x_1^* is an ESS we examine the behavior of dB'/dt near x_1^*. At the co-limitation point $x_1\alpha_1\bar{R}_1 = (1-x_1)\alpha_2\bar{R}_2$. When a mutant first appears, the system does not change appreciably, so $\bar{R}_1$ and $\bar{R}_2$ are unaffected by the appearance of mutant x_1's. Therefore, reducing or increasing x_1 will decrease growth, and thus no mutant can invade a co-limited resident. x_1^* is convergence and evolutionarily stable, so it is a continuously stable strategy (Eshel, 1983).

References

Abrams, P., 1987. The functional responses of adaptive consumers of two resources. Theor. Popul. Biol. 32 (2), 262–288.
Azam, F., Fenchel, T., Gray, J.G., Meyer-Reil, L.A., Thingstad, T., 1983. The ecological role of water-column microbes in the sea. Mar. Ecol. Prog. Ser. 10 (3), 257–263.
Ballantyne IV., F., Menge, D.N.L., Ostling, A., Hosseini, P., 2008. Nutrient recycling affects autotroph and ecosystem stoichiometry. Am. Nat. 171 (4), 511–523.
Barber, R.T., Chavez, F.P., 1983. Biological consequences of El Niño. Science 222, 1203–1210.
Bergh, Ø., Børsheim, K.Y., Bratbak, G., Heldal, M., 1989. High abundances of viruses found in aquatic environments. Nature 340, 467–468.

Böhm, J., Lambert, O., Frangakis, A.S., Letellier, L., Baumeister, W., Rigaud, J.L., 2001. FhuA-mediated phage genome transfer into liposomes: a cryo-electron tomography study. Curr. Biol. 11 (15), 1168–1175.
Borer, E.T., Halpern, B.S., Seabloom, E.W., 2006. Asymmetry in community regulation: effects of predators and productivity. Ecology 87 (11), 2813–2820.
Chapman-McQuiston, E., Wu, X.L., 2008. Stochastic receptor expression allows sensitive bacteria to evade phage attack: part I: experiments. Biophys. J. 94 (11), 4525–4536.
Cho, B.C., Azam, F., 1988. Major role of bacteria in biogeochemical fluxes in the oceans interior. Nature 332, 441–443.
DeAngelis, D.L., 1992. Dynamics of Nutrient Cycling and Food Webs. Chapman & Hall, London.
De Paepe, M., Taddei, F., 2006. Viruses' life history: towards a mechanistic basis of a trade-off between survival and reproduction among phages. PLoS Biol. 4 (7), e193.
Dukes, J.S., Chiariello, N.R., Cleland, E.E., Moore, L.A., Shaw, R.M., Thayer, S., Tobeck, T., Mooney, H.A., Field, C.B., 2005. Responses of grassland production to single and multiple global environmental changes. PLoS Biol. 3 (10), e319.
Elser, J.J., Bracken, M.S., Cleland, E.E., Gruner, D.S., Harpole, W.S., Hillebrand, H., Ngai, J.T., Seabloom, E.W., Shurin, J.B., Smith, J.E., 2007. Global analysis of nitrogen and phosphorus limitation of primary producers in freshwater, marine and terrestrial ecosystems. Ecol. Lett. 10 (12), 1135–1142.
Eshel, I., 1983. Evolutionary and continuous stability. J. Theor. Biol. 103 (1), 99–111.
Franks, P.J.S., 2002. NPZ models of plankton dynamics: their construction, coupling to physics, and application. J. Oceanogr. 58 (2), 379–387.
Fuhrman, J.A., 1999. Marine viruses and their biogeochemical and ecological effects. Nature 399, 541–548.
Gehring, K., Charbit, A., Brissaud, E., Hofnung, M., 1987. Bacteriophage λ receptor site on the *Escherichia coli* K-12 LamB protein. J. Bacteriol. 169 (5), 2103–2106.
Geritz, S.A.H., Metz, J.A.J., Kisdi, E., Meszena, G., 1997. Dynamics of adaptation and evolutionary branching. Phys. Rev. Lett. 78 (10), 2024–2027.
Gobler, C.J., Hutchins, D.A., Fisher, N.S., Cosper, E.M., 1997. Release and bioavailability of C, N, P, Se, and Fe following viral lysis of a marine chrysophyte. Limnol. Oceanogr. 42 (7), 1492–1504.
Hairston, N.G., Smith, F.E., Slobodkin, L.B., 1960. Community structure, population control, and competition. Am. Nat. 94, 421–425.
Holling, C.S., 1959. Some characteristics of simple types of predation and parasitism. Canad. Entomol. 91, 293–320.
Hunter, M.D., Varley, G.C., Gradwell, G.R., 1997. Estimating the relative roles of top-down and bottom-up forces on insect herbivore populations: a classic study revisited. Proc. Natl. Acad. Sci. USA 94 (17), 9176–9181.
Jaschinski, S., Sommer, U., 2008. Top-down and bottom-up control in an eelgrass-epiphyte system. Oikos 117 (5), 754–762.
Jiang, L., Schofield, O.M.E., Falkowski, P.G., 2005. Adaptive evolution of phytoplankton cell size. Am. Nat. 166 (4), 496–505.
Karl, D.M., Björkman, K.M., Dore, J.E., Fujieki, L., Hebel, D.V., Houlihan, T., Letelier, R.M., Tupas, L.M., 2001. Ecological nitrogen-to-phosphorus stoichiometry at station ALOHA. Deep-Sea Res. II 48 (8–9), 1529–1566.
Killmann, H., Videnov, G., Jung, G., Schwarz, H., Braun, V., 1995. Identification of receptor binding sites by competitive peptide mapping: phages T1, T5, and ϕ80 and Colicin M bind to the gating loop of FhuA. J. Bacteriol. 177 (3), 694–698.
Klausmeier, C.A., Litchman, E., Levin, S.A., 2004. Phytoplankton growth and stoichiometry under multiple nutrient limitation. Limnol. Oceanogr. 49 (4), 1463–1470.
Klausmeier, C.A., Litchman, E., Levin, S.A., 2007. A model of flexible uptake of two essential resources. J. Theor. Biol. 246 (2), 278–289.
Legović, T., Cruzado, A., 1997. A model of phytoplankton growth on multiple nutrients based on the Michaelis–Menten–Monod uptake, Droop's growth and Liebig's law. Ecol. Modelling 99 (1), 19–31.
Levin, S.A., Muller-Landau, H.C., 2000. The evolution of dispersal and seed size in plant communities. Evol. Ecol. Res. 2 (4), 409–435.
Levitus, S., Conkright, M.E., Reid, J.L., Najjar, R.G., Mantyla, A., 1993. Distribution of nitrate, phosphate, and silicate in the world oceans. Prog. Oceanogr. 31 (3), 245–273.
Li, W.K.W., 2002. Macroecological patterns of phytoplankton in the northwestern North Atlantic Ocean. Nature 419, 154–157.
Martin, J.H., Coale, K.H., Johnson, K.S., Fitzwater, S.E., Gordon, R.M., Tanner, S.J., Hunter, C.N., Elrod, V.A., Nowicki, J.L., Coley, T.L., Barber, R.T., Lindley, S., Watson, A.J., Van Scoy, K., Law, C.S., Liddicoat, M.I., Ling, R., Stanton, T., Stockel, J., Collins, C., Anderson, A., Bidigare, R., Ondrusek, M., Latasa, M., Millero, F.J., Lee, K., Yao, W., Zhang, J.Z., Friederich, G., Sakamoto, C., Chavez, F., Buck, K., Kolber, Z., Greene, R., Falkowski, P., Chisholm, S.W., Hoge, F., Swift, R., Yungel, J., Turner, S., Nightingale, P., Hatton, A., Liss, P., Tindale, N.W., 1994. Testing the iron hypothesis in ecosystems of the equatorial Pacific Ocean. Nature 371, 123–129.
May, R.M., 1973. Stability and Complexity in Model Ecosystems. Princeton University Press, Princeton, NJ.
Menge, B.A., 2000. Top-down and bottom-up community regulation in marine rocky intertidal habitat. J. Exp. Mar. Biol. Ecol. 250 (1–2), 257–289.
Menge, B.A., Daley, B.A., Wheeler, P.A., Dahlhoff, E., Sanford, E., Strub, P.T., 1997. Benthic-pelagic links and rocky intertidal communities: bottom-up effects on top-down control? Proc. Natl. Acad. Sci. USA 94 (26), 14530–14535.
Menge, B.A., Daley, B.A., Lubchenco, J., Sanford, E., Dahlhoff, E., Halpin, P.M., Hudson, G., Burnaford, J.L., 1999. Top-down and bottom-up regulation of New Zealand rocky intertidal communities. Ecol. Monogr. 69 (3), 297–330.
Menge, B.A., Lubchenco, J., Bracken, M.E.S., Chan, F., Foley, M.M., Freidenburg, T.L., Gaines, S.D., Hudson, G., Krenz, C., Leslie, H., Menge, D.N.L., Russell, R., Webster, M.S., 2003. Coastal oceanography sets the pace of rocky intertidal community dynamics. Proc. Natl. Acad. Sci. USA 100 (21), 12229–12234.
Menge, D.N.L., Levin, S.A., Hedin, L.O., 2008. Evolutionary tradeoffs can select against nitrogen fixation and thereby maintain nitrogen limitation. Proc. Natl. Acad. Sci. USA 105 (5), 1573–1578.
Moreau, G., Eveleigh, E.S., Lucarotti, C.J., Quiring, D.T., 2006. Ecosystem alteration modifies the relative strengths of bottom-up and top-down forces in a herbivore population. J. Anim. Ecol. 75 (4), 853–861.
Poorvin, L., Rinta-Kanto, J.M., Hutchins, D.A., Wilhelm, S.W., 2004. Viral release of iron and its bioavailability to marine plankton. Limnol. Oceanogr. 49 (5), 1734–1741.
Proctor, L.M., Fuhrman, J.A., 1990. Viral mortality of marine bacteria and cyanobacteria. Nature 343, 60–62.
Proctor, L.M., Fuhrman, J.A., 1992. Mortality of marine bacteria in response to enrichments of the virus size fraction from seawater. Mar. Ecol. Prog. Ser. 87 (3), 283–293.
Redfield, A.C., 1958. The biological control of chemical factors in the environment. Am. Sci. 46 (3), 205–221.
Reynolds, H.L., Pacala, S.W., 1993. An analytical treatment of root-to-shoot ratio and plant competition for soil nutrient and light. Am. Nat. 141 (1), 51–70.
Rosenzweig, M.L., MacArthur, R.H., 1963. Graphical representation and stability conditions of predator–prey interactions. Am. Nat. 97, 209–223.
Suttle, C.A., 1992. Inhibition of photosynthesis in phytoplankton by the submicron size fraction concentrated from seawater. Mar. Ecol. Prog. Ser. 87 (1–2), 105–112.
Suttle, C.A., 2005. Viruses in the sea. Nature 437, 356–360.
Suttle, C.A., Chan, A.M., Cottrell, M.T., 1990. Infection of phytoplankton by viruses and reduction of primary productivity. Nature 347, 467–469.
Tilman, D., 1982. Resource Competition and Community Structure. Princeton University Press, Princeton, NJ.
Tyrrell, T., 1999. The relative influences of nitrogen and phosphorus on oceanic primary production. Nature 400, 525–531.
Van den Berg, H.A., Kiselev, Y.N., Orlov, M.V., 2002. Optimal allocation of building blocks between nutrient uptake systems in a microbe. J. Math. Biol. 44 (3), 276–296.
Vitousek, P.M., Farrington, H., 1997. Nutrient limitation and soil development: experimental test of a biogeochemical theory. Biogeochemistry 37 (1), 63–75.
Vitousek, P.M., Howarth, R.W., 1991. Nitrogen limitation on land and sea: How can it occur? Biogeochemistry 13 (2), 87–115.
Volterra, V., 1926. Fluctuations in the abundance of a species considered mathematically. Nature 118, 558–560.
Weinbauer, M.G., 2004. Ecology of prokaryotic viruses. FEMS Microbiol. Rev. 28 (2), 127–181.
Weitz, J.S., Hartman, H., Levin, S.A., 2005. Coevolutionary arms races between bacteria and bacteriophage. Proc. Natl. Acad. Sci. USA 102 (27), 9535–9540.
Wilhelm, S.W., Suttle, C.A., 1999. Viruses and nutrient cycles in the sea. BioScience 49 (10), 781–788.
Wommack, K.E., Colwell, R.R., 2000. Virioplankton: viruses in aquatic ecosystems. Microbiol. Mol. Biol. Rev. 64 (1), 69–114.